JOURNAL OF VIROLOGY, Jan. 2011, p. 21–31 Vol. 85, No. 1
0022-538X/11/$12.00 doi:10.1128/JVI.01814-10

Variola and Monkeypox Viruses Utilize Conserved Mechanisms of Virion Motility and Release That Depend on Abl and Src Family Tyrosine Kinases▽†

Patrick M. Reeves,[1] Scott K. Smith,[3] Victoria A. Olson,[3] Steve H. Thorne,[4] William Bornmann,[2] Inger K. Damon,[3] and Daniel Kalman[1,5]*

Microbiology and Molecular Genetics Graduate Program, Emory University School of Medicine, 615 Michael Street, Whitehead Research Building 155, Atlanta, Georgia 30322[1]; M. D. Anderson Cancer Center, University of Texas, Houston, Texas[2]; Poxvirus Team, Poxvirus and Rabies Branch, Division of Viral and Rickettsial Diseases, National Center for Zoonotic, Viral and Enteric Diseases, Centers for Disease Control and Prevention, Atlanta, Georgia 30333[3]; Division of Surgical Oncology and Department of Immunology, Hillman Cancer Center, University of Pittsburgh Cancer Institute, Pittsburgh, Pennsylvania 15213[4]; and Department of Pathology and Laboratory Medicine, Emory University School of Medicine, 615 Michael Street, Whitehead Research Building 144, Atlanta, Georgia 30322[5]

Received 26 August 2010/Accepted 5 October 2010

Vaccinia virus (VacV) enters mammalian cells, replicates extranuclearly, and produces virions that move to the cell surface along microtubules, fuse with the plasma membrane, and move from infected cells toward apposing cells on actin-filled membranous protrusions or actin tails. To form actin tails, cell-associated enveloped virions (CEV) require Abl and Src family tyrosine kinases. Furthermore, release of CEV from the cell requires Abl but not Src family tyrosine kinases and is blocked by imatinib mesylate (STI-571; Gleevec), an Abl family kinase inhibitor used to treat chronic myelogenous leukemia in humans. Here we demonstrate that the *Poxviridae* family members monkeypox virus (MPX) and variola virus (VarV) use conserved mechanisms for actin motility and extracellular enveloped virion (EEV) release. Furthermore, we show that imatinib mesylate is effective in a mouse model of infection with VacV, whether delivered prophylactically or postinfection, and restricts spread of virions from the site of inoculation. While inhibitors of both Src and Abl family kinases, such as dasatinib (BMS-354825; Sprycel), are effective in limiting dissemination of VacV, VarV, and MPX *in vitro*, members of this class of drugs appear to have immunosuppressive effects *in vivo* that preclude their use as anti-infectives. Together, these data suggest a possible utility for imatinib mesylate in treating smallpox or MPX infections or complications associated with vaccination.

Vaccinia virus (VacV), monkeypox virus (MPX), and variola virus (VarV) are members of the *Poxviridae* orthopoxvirus family (9, 17). Vaccination with VacV provides protection against MPX and VarV, the cause of smallpox. Routine vaccinations for smallpox ceased in 1977, and smallpox was declared eradicated by the World Health Organization (WHO) in 1980. Estimates indicate that about half of the individuals in the general population are not vaccinated (19). As such, the general population is considered extremely susceptible to a smallpox outbreak resulting from release of the virus. Moreover, recent outbreaks of MPX in the United States and in the Democratic Republic of Congo have raised the prospect that emergent poxviruses may also pose a significant threat (7, 21).

Vaccination, even postexposure, is still considered the method of choice for treatment of orthopoxvirus infections. However, the window for efficacious postexposure vaccination is small (~4 to 7 days) (16). Moreover, individuals with acquired or congenital immunocompromising conditions appear to be at high risk for developing complications upon vaccination (5, 6), which include encephalitis, fetal vaccinia, progressive vaccinia, and eczema vaccinatum, a localized or systemic dissemination of the virus (6, 19, 34).

The mechanisms of VacV entry into host cells, replication, and exit have been studied extensively (17). Upon entry, the virion moves to a juxtanuclear location, where it replicates up to 10^4 concatemeric genomes, which resolve into individual unit genomes and then are packaged into virions (called intracellular mature virions [IMV]). Some IMV are packaged in additional membranes to form intracellular enveloped virions (IEV), which travel toward the host cell periphery via a kinesin/microtubule transport system (4, 11, 22, 25) and fuse with the plasma membrane of the host cell to form cell-associated enveloped virions (CEV), leaving behind one of the two outer membranes (17, 27, 28). CEV can initiate actin polymerization, which propels the particle on an actin-filled membrane protuberance (called a "tail") toward an adjacent cell. CEV can detach from the tip of a tail or directly from the membrane (27) to form extracellular enveloped virions (EEV) (28). EEV are assessed *in vitro* as "comets," consisting of an archipelago of secondary satellite plaques apposed to a larger plaque (28). EEV have been proposed to mediate long-range spread of the virus *in vivo* (28). Experiments with VacV have demonstrated

* Corresponding author. Mailing address: Department of Pathology and Laboratory Medicine, Emory University, Whitehead Research Bldg. 144, 165 Michael St., Atlanta, GA 30322. Phone: (404) 712-2326. Fax: (404) 712-2979. E-mail: dkalman@emory.edu.

† Supplemental material for this article may be found at http://jvi.asm.org/.

▽ Published ahead of print on 20 October 2010.

that Src and Abl family kinase activities modulate intracellular spread and release (10a, 24). In particular, phosphorylation of tyrosine residues of A36R, a viral protein in the outer membrane of IEV, by Abl or Src family kinases is required for recruitment of Nck, Grb2, and the Arp2/3 complex, molecules that stimulate actin polymerization and tail formation (19a, 26). Abl family kinases, but not Src family kinases, also mediate release of CEV to form EEV (24).

The proposed dependence of VacV dissemination *in vivo* upon release of EEV (28) and the requirement for Abl family tyrosine kinases in EEV release (24) raised the possibility that tyrosine kinase inhibitors originally developed for treating cancers may also have utility as therapeutics for infections caused by many poxviruses. Imatinib mesylate (STI-571; Gleevec), nilotinib mesylate (AMN-107; Tasigna), and the related small-molecule inhibitor dasatinib (BMS-354285; Sprycel) are all approved for treating human cancers, including chronic myelogenous leukemia (CML) and gastrointestinal stromal tumors (32, 35). Imatinib mesylate and nilotinib mesylate inhibit Abl family kinases, whereas dasatinib and another structurally related compound, PD-166236, inhibit both Src and Abl family kinases. Notably, imatinib mesylate reduces VacV dissemination *in vivo* and provides protection from an otherwise lethal infection when delivered prophylactically (24).

Although VarV, MPX, and VacV genomes have been sequenced and are 95% identical (9), there is no evidence that MPX and VarV form actin tails and release EEV by using the same host molecules as VacV. The data presented here suggest that these mechanisms are highly conserved among poxviruses. We also tested the hypothesis that tyrosine kinase inhibitors approved for use in humans, such as imatinib mesylate and dasatinib, may have utility against poxvirus infections *in vivo*. We report here that imatinib mesylate is effective in both prophylactic and therapeutic capacities against VacV infections in mice and limits spread of the virus from the site of inoculation. Moreover, imatinib mesylate does not interfere with the acquisition of protective immunity. In contrast, while dasatinib has strong efficacy *in vitro* against all poxviruses tested, immunosuppressive effects *in vivo* appear to preclude its use as a therapeutic agent. Together, these data provide an experimental basis for the development of small-molecule tyrosine kinase inhibitors for poxvirus infections.

MATERIALS AND METHODS

Cells and viruses. African green monkey kidney cells (BSC-40) and murine fibroblast cells (3T3, $Src^{-/-}$ $Fyn^{-/-}$ $Yes1^{-/-}$, and $Abl1^{-/-}$ $Abl2^{-/-}$ cells) were cultured as described previously (31). For VacV experiments, cells were maintained in Dulbecco's modified Eagle's medium (DMEM) supplemented with 10% fetal bovine serum (FBS), penicillin, and streptomycin (complete medium) as described previously (31). For MPX and VarV experiments, BSC-40 cells were cultured as described previously (29). Viruses were obtained from crude lysate preparations of infected BSC-40 cells as described previously (29). For these experiments, we used VacV strains WR and IHD-J, MPX strain MPXV-1979-ZAI-005, and VarV strains BSH74-sol (BSH; Bangladesh) and SLN68-258 (SLN; Sierra Leone). VacV and MPX experiments were conducted under appropriate biosafety conditions. Assays with VarV were performed in a maximum containment laboratory under biosafety level 4 (BSL4) conditions. For microscopy, murine fibroblast 3T3, $Src^{-/-}$ $Fyn^{-/-}$ $Yes1^{-/-}$, or $Abl1^{-/-}$ $Abl2^{-/-}$ cells were cultured on glass coverslips in complete medium and then incubated with virus at a multiplicity of infection (MOI) of 5 for 1 h in DMEM lacking serum. The cells were then washed and incubated in complete medium. After 18 to 24 h, cells were fixed and prepared for immunofluorescence as described below.

Immunofluorescence analysis. Cells previously infected with VacV, MPX, or VarV were fixed in 2% paraformaldehyde and permeabilized in 0.1% Triton X-100 as described previously (13). Viral DNA was recognized by staining with DAPI (4′,6-diamidino-2-phenylindole; 1 μg/ml) (Sigma), and actin was visualized by staining with 488-phalloidin (1 μg/ml; Molecular Probes). The primary antibodies and concentrations used in this study were as follows: Nck monoclonal antibody (MAb) (1 μg/ml; Oncogene Research), Abl1 MAb (8E9) (0.05 μg/ml; Pharmingen), Src polyclonal antibody (PAb) (0.1 μg/ml; Santa Cruz), Fyn MAb (0.1 μg/ml; Abcam), Yes PAb (0.1 μg/ml; Cell Signaling), Abl2 PAb (1:200; UBI), Grb2 MAb (3F2) (1:200), and phosphotyrosine MAb (4g10) (1:200); the specificity of anti-kinase antibodies was confirmed by staining cell lines lacking particular kinases (24). Secondary antibodies were obtained from Jackson Immunochemicals. Following fixation, VarV samples were stained with DAPI (1 μg/ml; Sigma) and 488-phalloidin (10 μg/ml; Molecular Probes). The samples were then inactivated with 3% Amphyll for 30 min in accordance with the guidelines of the Office of Health and Safety at the Centers for Disease Control and Prevention (CDC). Samples were then removed from the BSL4 facility, washed three times with phosphate-buffered saline (PBS), and stained and imaged as described here.

Microscopy. Images were acquired with a scientific-grade cooled charge-coupled device (Cool-Snap HQ with ORCA-ER chip) on a multiwavelength widefield three-dimensional microscopy system (Intelligent Imaging Innovations) based on a Zeiss 200 M inverted microscope using a 63×, 1.4-numerical aperture (NA) or 100×, 1.4-NA lens (Zeiss). Imaging of immunofluorescent samples was done at room temperature (22 to 25°C), using a standard Sedat filter set (Chroma) in successive 0.20-μm focal planes through the samples, and out-of-focus light was removed with a constrained iterative deconvolution algorithm (30). Actin tails were recognized by intense phalloidin staining associated with DAPI or green fluorescent protein (GFP) fluorescent objects measuring approximately 200 nm in diameter. Fluorescence at the ends of actin tails which colocalized with DAPI staining or with GFP fluorescence in cells infected with GFP-labeled VacV was used to indicate localization of kinases or other cellular molecules to virions. Colocalization was assessed by coincidence of fluorescence staining of kinases in the Cy5 and Cy3 channels. We calibrated the microscope filters with multicolored fluorescent beads to ensure coincidence of fluorescent signals in all channels to within a pixel (100 nm for the 63×, 1.4-NA lens).

***In vivo* drug delivery and mouse assays.** Synthesis and delivery of imatinib mesylate were achieved as described previously (24). Briefly, 200 mg of drug/kg of body weight/day was delivered via Alzet osmotic pumps inserted subcutaneously into anesthetized 6-week-old female C57/BL6 mice. BMS-354825 was suspended in 50% DMSO-H_2O at various concentrations (noted in the figure legends) and delivered into animals by osmotic pumps. Mice were infected either intraperitoneally (i.p.) or intranasally (i.n.) with 10^4 PFU VacV IHD-J as previously reported (24). To measure viral copy numbers, organs were harvested at 4 days postinfection and prepared as previously described (24). For survival studies, mice were sacrificed at 70% of their original weight or as directed by veterinary staff. Mice were monitored daily, and all experiments were carried out in accordance with Institutional Animal Care and Use Committee regulations (Emory University protocol number AD07-1156-03R04 or University of Pittsburgh regulations). In some studies, mice received 10^2 PFU of IHD-J expressing luciferase and viral gene expression was monitored using bioluminescence imaging. Mice were injected with 30 mg/kg luciferin and anesthetized (2% isoflurane) before being imaged in an IVIS200 instrument (Xenogen; part of Caliper Life Science), and images were analyzed using Living Image software.

Viral copy number measurements. Viral genome copy number measurements were carried out as described previously (24). Probes and primers were obtained from Operon Biotechnologies. TaqMan probe analysis was conducted on a Roche Lightcycler 480, utilizing a standard curve for absolute quantification.

Plaque assays and IHC. Plaque assays were conducted as described previously, with minor modifications (36). BSC-40 cells were seeded in six-well plates and grown to confluence. VacV, MPX, or VarV was diluted in RPMI containing 2% FBS, and ~25 PFU was added to each well. Following 1 h of incubation with virus, imatinib mesylate, nilotinib mesylate, dasatinib, or PD-166326 was added to final concentrations of 0.05 to 10 μM. Immunohistochemistry (IHC) was performed as described previously (8, 36). Briefly, cells were incubated with polyclonal rabbit anti-variola virus antibody and goat anti-rabbit immunoglobulin G–horseradish peroxidase conjugate (KPL 074-1506; Kirkegaard & Perry Laboratories). The plaques were visualized by development with TrueBlue peroxidase substrate (KPL 71-00-64; Kirkegaard & Perry Laboratories). Assays with VarV were performed in a maximum containment laboratory under BSL4 conditions. Six-well plates containing VarV were double sealed in Kapak/Scotchpak pouches and gamma irradiated at the kill dose of 4.4×10^6 rads prior to IHC staining (19).

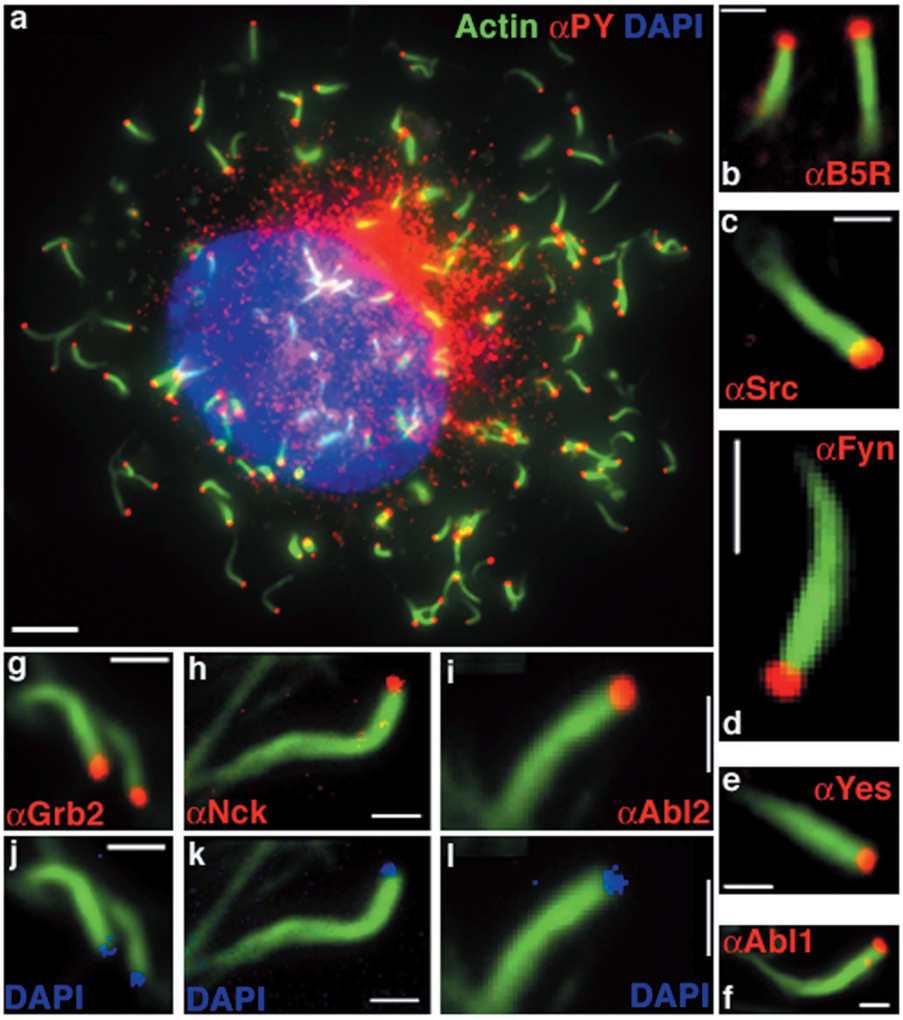

FIG. 1. VarV recruits host cell factors required for actin polymerization. (a) Image of 3T3 cell infected with VarV-BSH and stained with FITC-phalloidin to visualize actin (green), with pY MAb (red), and with DAPI to visualize DNA (blue). (b to i) Images of actin tails on 3T3 cells infected with VarV strain BSH or SLN and stained with FITC-phalloidin (green) and the following antibodies against cellular and viral proteins (red): B5R MAb (b), Src PAb (c), Fyn MAb (d), Yes MAb (e), Abl1 MAb (f), Grb2 PAb (g), Nck MAb (h), and Abl2 MAb (i). Panels j to l depict DAPI staining (blue) at the tips of tails from panels g to i. Bars, 5 μm (a) and 1 μm (b to i).

Comet assays. Confluent monolayers of BSC-40 wells in 6-well dishes were infected with ~25 PFU of VacV-WR, MPX, or VarV-BSH diluted in 2% FBS-RPMI. The comet assay was performed as described previously (8, 24), with some modifications. The cells, viral dilutions, infection procedures, drug concentrations, gamma irradiation for VarV, and IHC were as described above for the plaque size evaluation assay. During the 2-, 3-, or 4-day incubation period for VacV, MPX, or VarV, respectively, the plates were placed at a fixed angle of approximately 5 degrees and then fixed and stained with antibody as described previously (8, 36).

EEV quantification assays. Methods for quantification of EEV have been described previously (24). Briefly, 6-well dishes were seeded with BSC-40 cells, which were allowed to grow to ~90% confluence. Cells were then incubated with VacV, MPX, or VarV at an MOI of either 5 or 0.1. The supernatants were harvested at 18 to 24 h postinfection and were incubated with IMV neutralizing antibody for 1 h. To quantify the remaining infectious particles, serial dilutions of the neutralized supernatant were incubated with naïve BSC-40 cell monolayers. After 1 h, media were exchanged, and 2, 3, and 4 days later, for VacV, MPX, and VarV, respectively, cells were stained with 1% crystal violet and plaques enumerated. To enumerate cell-associated virions (CAV), cells were plated and infected as described above. After 24 h, cells were scraped and lysed by freeze-thawing. Serial dilutions of the supernatant were incubated with BSC-40 monolayers for 1 h, the media were exchanged, and 2, 3, or 4 days later, for VacV, MPX, or VarV, respectively, cells were stained with 1% crystal violet and plaques enumerated.

Construction of IHD-J luciferase-expressing virus. VacV IHD-J expressing luciferase (IHD-J Luc) was constructed using IHD-J ΔVP37 and firefly luciferase. The luciferase gene was amplified by PCR with *Pfu* Turbo (Stratagene, La Jolla, CA), using primers 5′GCGC*GAATTC*ATGGAAGACGCCAAAAACAT AAAGAAAG3′ and 5′GCGC*AAGCTT*TTACACGGCGATCTTTCCGCC 3′, from plasmid pGL3 to generate a 1,673-bp fragment with EcoRI and HindIII sites added (restriction sites are shown in italics). The PCR product was inserted into pRB21 (a gift from Bernie Moss) at EcoRI and HindIII sites to create pRB21-LUC. CV-1 cells were infected with 10^6 PFU/ml IHD-J ΔVP37 and transfected with 2 μg of pRB21-LUC by use of Fugene (Roche, Indianapolis, IN). After 48 h, the resulting virus was harvested from the cell medium. Recombinant virus was isolated by applying CV-1 supernatant to naïve CV-1 cells, overlaying monolayers with 1.5% agarose, and screening for large plaques. Plaques were selected and plaque purified 3 times on CV-1 cells to isolate IHD-J Luc. Luciferase insertion was confirmed by PCR with primers 5′GCGC*GAATT C*ATGGAAGACGCCAAAAACATAAAGAAAG3′ and 5′GCGC*AAGCTT*TT ACACGGCGATCTTTCCGCC3′ to generate a 1,673-bp product, which was sequenced with primers 5′TTTGAGAGAGATTGGGTGAGCTCACATTC3′ and 5′AGGTTTGTATCCTGTTTAACATGATGGCG3′. Luciferase activity was confirmed *in vitro* by infecting CV-1 cells with 10^6 PFU/ml IHD-J Luc for 1

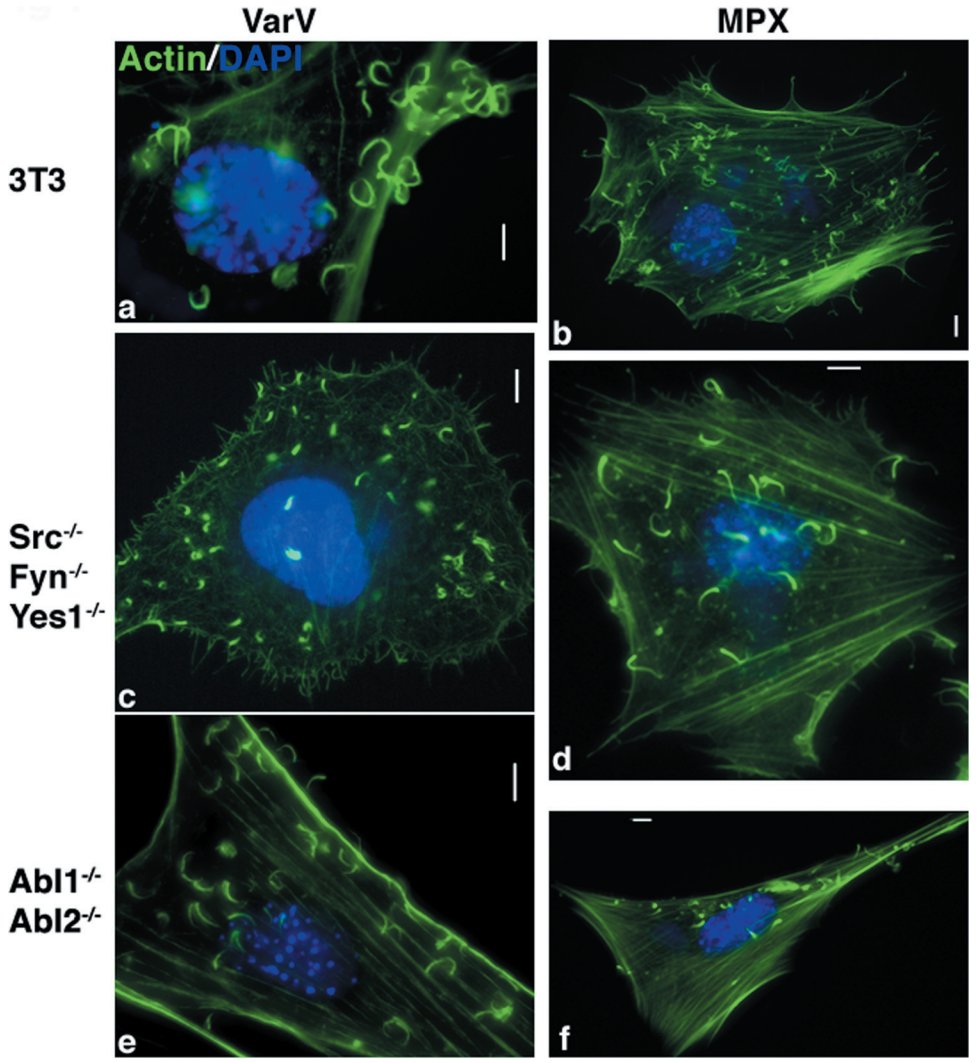

FIG. 2. VarV and MPX form actin tails. (a to f) Images of fibroblast cell lines derived from WT mice (3T3) (a and b), $Src^{-/-}$ $Fyn^{-/-}$ $Yes1^{-/-}$ mice (c and d), and $Abl1^{-/-}$ $Abl2^{-/-}$ mice (e and f), infected with VarV strain BSH (a, c, and e) or with MPX (b, d, and f) for 24 h, fixed, and stained with DAPI (blue) and FITC-phalloidin (green) to recognize DNA and actin, respectively. Bars, 5 μm.

day and analyzing luciferase activity with the Bright-Glo luciferase assay system (Promega, Madison, WI).

RESULTS

Actin motility in VarV and MPX. To determine whether the orthopoxviruses VacV, MPX, and VarV use common mechanisms of actin motility, the capacity of these viruses to induce actin tails in infected cells was assessed. 3T3 mouse fibroblasts were infected with either VarV or MPX and then fixed and stained with fluorescein isothiocyanate (FITC)-phalloidin to recognize actin and with DAPI to recognize DNA. Both VarV and MPX formed actin-filled membranous protrusions ("tails") in infected cells (Fig. 1a; also see Fig. 2 and see Fig. S1a in the supplemental material). VarV and MPX actin tails appeared generally similar to those of VacV (see Fig. S2a), though some subtle morphological differences were evident. For example, MPX occasionally induced the formation of "doublet" tails, consisting of two fused tails with two virions at the tip (see Fig. S1b), and variola virus induced "horseshoe" tails (Fig. 2a and e), morphologies that were not apparent in cells infected with VacV (e.g., see Fig. S2a).

The complement of proteins at the tips of VarV and MPX actin tails was identical to that seen with VacV. Thus, phosphotyrosine (pY) staining and the virus-specific antigen B5R were evident at the tips of tails (Fig. 1a and b; see Fig. S1a and b in the supplemental material). Likewise, the tyrosine kinases Src, Fyn, Yes1, Abl1, and Abl2 and the accessory proteins Nck and Grb2, which are required for actin motility in VacV, all localized to the tips of VarV and MPX actin tails (Fig. 1c to i; see Fig. S1c to i). In some samples, DAPI staining at the tips of actin tails colocalized with Grb2, Nck, and Abl2 (Fig. 1j to l). Together, these data indicate that VarV and MPX recruit cellular proteins in a manner analogous to that of VacV.

Redundant Abl and Src family tyrosine kinases mediate VarV and MPX actin motility. To determine whether Src and Abl family kinase activities are required by VarV and MPX to

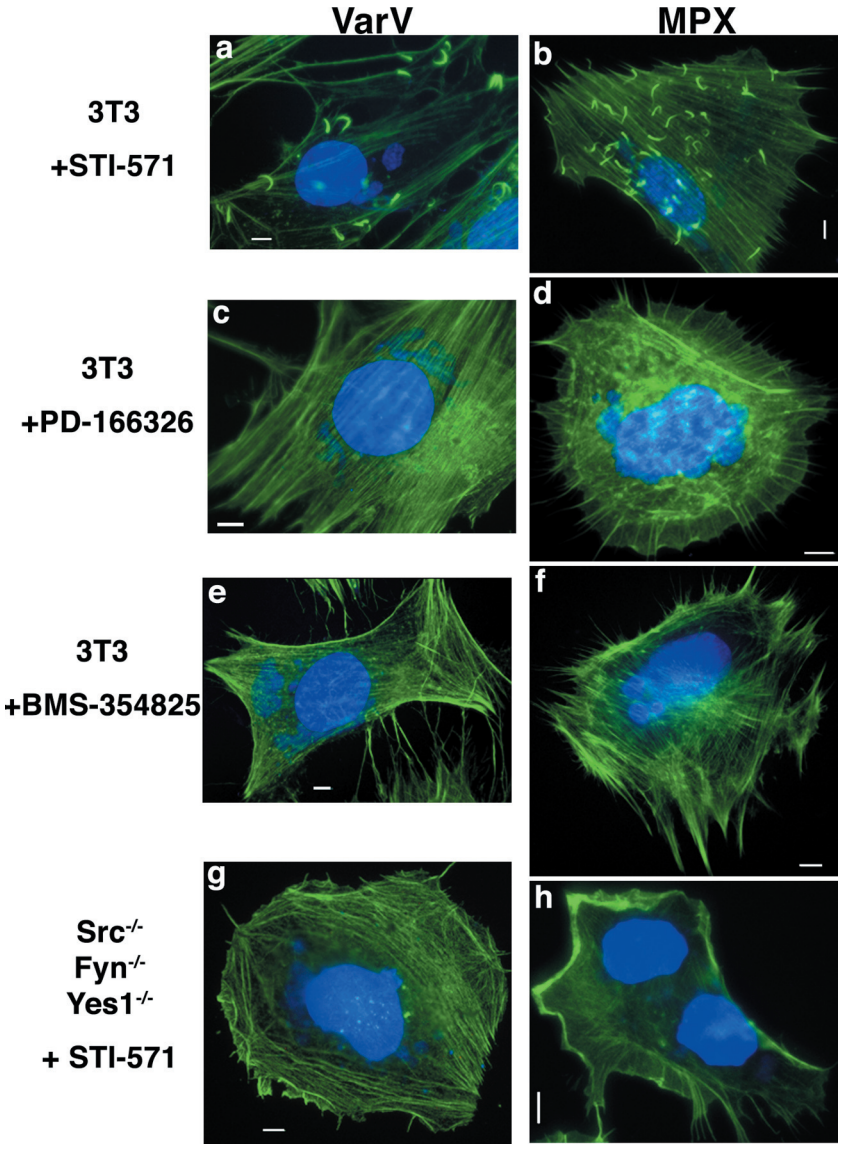

FIG. 3. Actin tails formed by VarV and MPX require Abl and Src family tyrosine kinases. (a to h) Images of fibroblast cell lines derived from WT mice (3T3) (a to f) and $Src^{-/-}$ $Fyn^{-/-}$ $Yes1^{-/-}$ mice (g and h) infected with VarV strain BSH (a, c, e, and g) or with MPX (b, d, f, and h) for 24 h, treated with imatinib mesylate (STI-571) (a, b, g, and h), PD-166326 (c and d), or dasatinib (BMS-354285) (e and f), each at 10 μM, and then fixed and stained with DAPI (blue) and FITC-phalloidin (green) to recognize DNA and actin, respectively. Bars, 5 μm.

form actin tails, we first assessed the capacity of MPX and VarV to form actin tails in 3T3 cells derived from animals lacking Src, Fyn, and Yes1 ($Src^{-/-}$ $Fyn^{-/-}$ $Yes1^{-/-}$) or from animals lacking Abl1 and Abl2 ($Abl1^{-/-}$ $Abl2^{-/-}$). VarV and MPX induced comparable actin tails in 3T3 cells (Fig. 2a and b), $Src^{-/-}$ $Fyn^{-/-}$ $Yes1^{-/-}$ cells (Fig. 2c and d), and $Abl1^{-/-}$ $Abl2^{-/-}$ cells (Fig. 2e and f), in accordance with previous observations with VacV (24). We next determined the effects of two classes of tyrosine kinase inhibitors on actin tails formed by VarV or MPX. Imatinib mesylate and nilotinib mesylate inhibit Abl family tyrosine kinases, whereas PD-166326 and dasatinib inhibit both Abl and Src family kinases. As with VacV, treatment of 3T3 cells with imatinib mesylate (10 μM) did not prevent actin tail formation by VarV or MPX (Fig. 3a and b) (24). However, no actin tails were evident in cells treated with either PD-166326 or dasatinib (Fig. 3c to f; see Fig. S2b in the supplemental material) (24). Notably, neither MPX nor VarV induced actin tails in $Src^{-/-}$ $Fyn^{-/-}$ $Yes1^{-/-}$ cells treated with imatinib mesylate (Fig. 3g and h). Collectively, these data indicate that VarV and MPX can utilize Abl or Src family tyrosine kinase activity to form actin tails. Moreover, like the case for VacV, usage of these kinases by VarV or MPX appears to be functionally redundant, that is, any one kinase can suffice in the absence of others.

Effects of tyrosine kinase inhibitors on CAV and EEV. We next tested the effects of tyrosine kinase inhibitors on formation of plaques and associated "comets," which are indicators of released EEV. Following adsorption with VacV, MPX, or VarV, BSC-40 cells were treated with the Src and Abl family inhibitors PD-166326 and dasatinib or the Abl family inhibitors

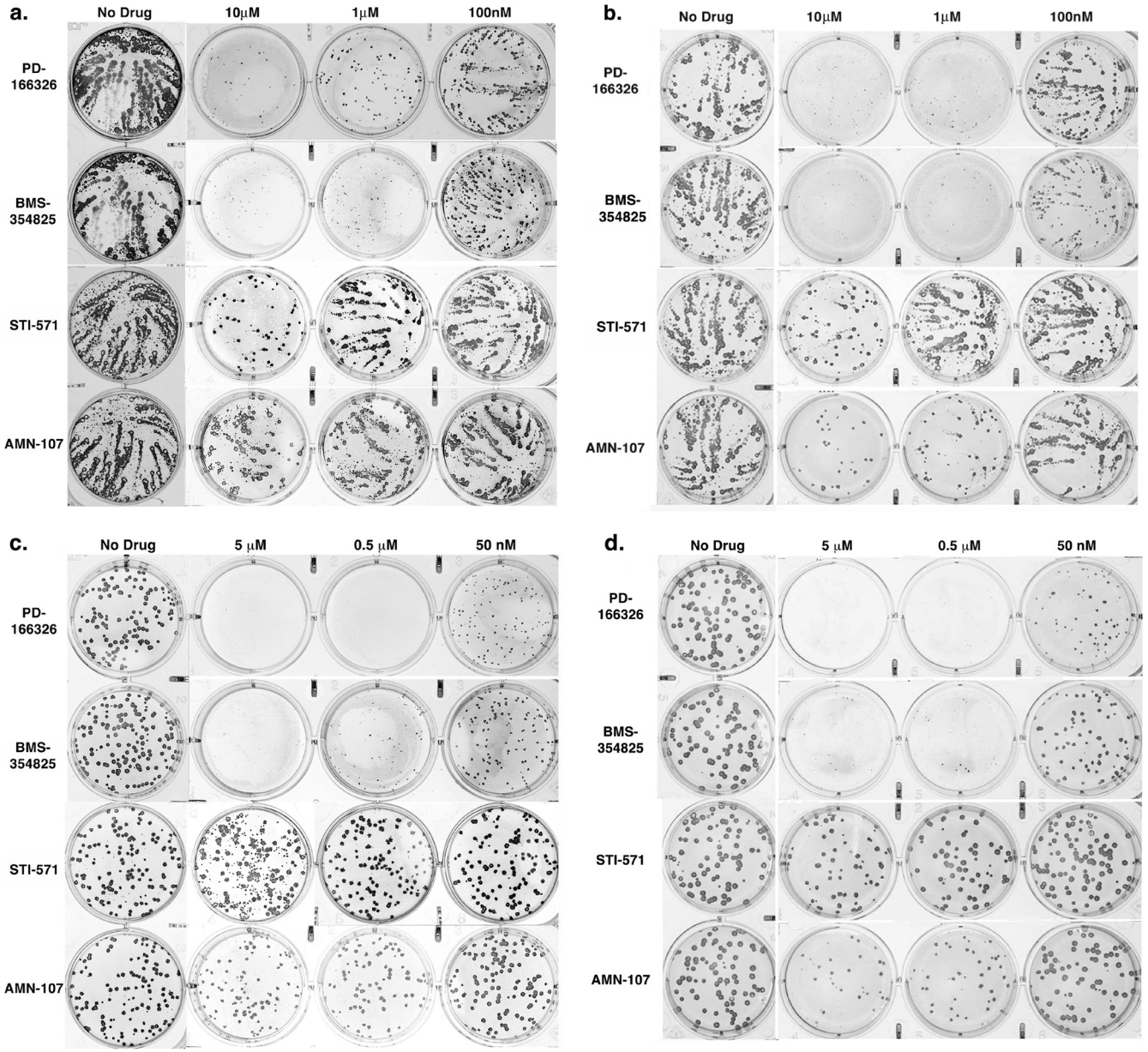

FIG. 4. Comet and CMC plaque assays. BSC-40 cells were infected with VarV strain BSH (a) or with MPX (b). Cells were left untreated or treated with either PD-166326, dasatinib (BMS-354825), imatinib mesylate (STI-571), or nilotinib mesylate (AMN-107) at 10 μM, 1 μM, or 100 nM. Drugs were added 1 h after infection. Cells were incubated for 4 days, fixed, and stained with VarV PAb to recognize infected cells. For carboxymethyl cellulose plaque assays, BSC-40 cells were infected with VarV strain BSH (c) or with MPX (d) and overlaid with CMC. PD-166326, dasatinib (BMS-354825), imatinib mesylate (STI-571), or nilotinib melsylate (AMN-107) was added to a final concentration of 5 μM, 0.5 μM, or 50 nM 1 h after infection. Cells were incubated for 4 days, fixed, and stained with a VarV PAb to recognize infected cells.

imatinib mesylate and nilotinib mesylate, at various concentrations. Cells were fixed after 48, 72, and 96 h for VacV, MPX, and VarV, respectively, and stained with a poxvirus PAb to identify infected cells. PD-166326 or dasatinib at concentrations of 1 to 10 μM reduced plaque size in cells infected with VarV-BSH, MPX, or VacV strains IHD-J and WR (Fig. 4; see Fig. S3 in the supplemental material) (24), and no "comets" were evident. In contrast, both imatinib mesylate and nilotinib mesylate reduced "comets" at a concentration of 10 μM but had no effect on plaque size (Fig. 4; see Fig. S3).

To more carefully assess the effects of drugs on actin motility and plaque size and to reduce the contribution of EEV to plaque size, we next carried out carboxymethyl cellulose (CMC) overlay experiments. CMC medium restricts the movement of released particles, thereby eliminating comets. Following the initial incubation with either VarV strain BSH or MPX, the inoculum medium was replaced with CMC medium containing either PD-166326, dasatinib, imatinib mesylate, or nilotinib mesylate at various concentrations. Under these conditions, PD-166326 and dasatinib reduced plaque size, whereas

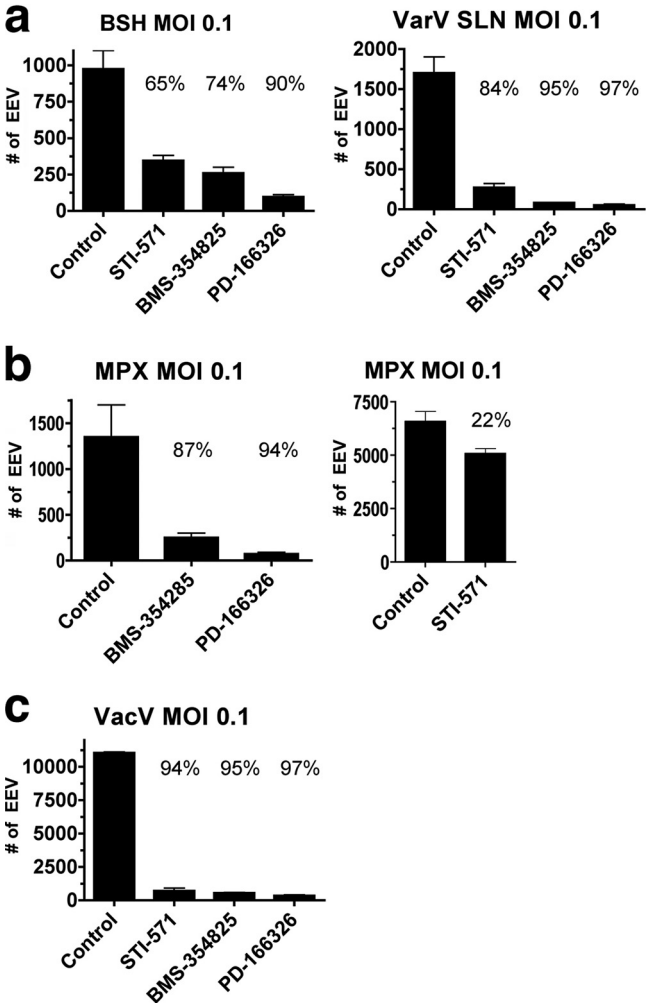

FIG. 5. Quantification of EEV from supernatant of BSC-40 cells infected with VarV strain BSH or strain SLN (a), with MPX (b), or with VacV strain WR (c) at an MOI of 0.1. The inoculum was removed at 1 h postinfection and replaced with medium containing imatinib mesylate (STI-571), dasatinib (BMS-354285), or PD-166326 (10 μM). After 24 h, the supernatant was removed, and cells were lysed and their titers measured on naïve BSC-40 cells.

imatinib mesylate and nilotinib mesylate had no effect compared to untreated controls, in accordance with the microscopy and comet assays (Fig. 4c and d).

To quantify the effects of drugs on EEV, we enumerated the number of virions released from BSC-40 cells infected at an MOI of 0.1 into the supernatant, as well as the total amount of CAV produced. Cell supernatants were harvested at 18 to 24 h postinfection, the time at which EEV release is maximal. Supernatants were then treated with IMV MAb (2D5 or L1R), and the released virus was titrated on naïve cells. Imatinib mesylate reduced the amount of EEV by 65%, 84%, 22%, and 94% for VarV-BSH, VarV-SLN, MPX, and VacV-WR, respectively (Fig. 5a, b, and c). Dasatinib and PD-166326 produced similar effects on EEV produced by VacV, MPX, VarV-BSH, and VarV-SLN (Fig. 5a, b, and c). None of the compounds affected production of CAV (not shown), with the exception of PD-166326, which caused a slight diminution, in accordance with previous findings (24). Collectively, these data suggest that inhibition of Abl family kinase activity reduced the amount of EEV, but not CAV, produced by VarV, MPX, and VacV.

Effects of tyrosine kinase inhibitors on VacV infections *in vivo*. Based on the capacity of dasatinib to prevent the formation of actin tails and reduce the amount of EEV, we tested whether administration of the drug could afford protection in mice challenged with an otherwise lethal inoculum of VacV. Beginning 24 h prior to infection, dasatinib was administered either by twice-daily injections or by an osmotic pump implanted subcutaneously to deliver drug at a constant rate for the duration of the experiment. Mice were then challenged i.n. with 2×10^4 PFU of VacV strain IHD-J, the lethal dose for 100% of mice (LD_{100}). No dose of dasatinib or delivery condition tested provided any survival benefit to the mice compared to PBS controls (Fig. 6a).

To investigate the capacity of dasatinib to limit dissemination, mice were implanted with osmotic pumps for delivery of drugs and then challenged with sublethal inocula of VacV IHD-J (2×10^4 PFU i.p.) Concentrations tested ranged between 0.05 and 240 mg/kg/day. After 4 days, the ovaries were removed, and viral genome copies were quantified by quantitative PCR. The data indicated that none of the doses of dasatinib within the range tested significantly reduce viral loads in mice (see Fig. S4a in the supplemental material). During postmortem analysis, spleens of mice treated with dasatinib appeared significantly reduced in weight relative to those of infected controls ($P = 0.001$) (see Fig. S4b). Taken together, these data suggested that dasatinib may negatively impact the immune response. To test this possibility directly, viral loads were assessed in ovaries of mice infected with a sublethal inoculum of VacV IHD-J (2×10^4 PFU i.p.) and treated with imatinib mesylate (200 mg/kg/day) together with dasatinib at either 0.5 or 0.05 mg/kg/day. As controls, we tested the effects of PBS, imatinib mesylate alone (200 mg/kg/day), or dasatinib alone, at either 0.05 or 0.5 mg/kg/day. In accordance with previous work, imatinib mesylate reduced the number of viral genome copies by ~4 log (Fig. 6b) (24). In contrast, dasatinib alone, at either 0.5 mg/kg/day or 0.05 mg/kg/day, reduced the number of viral genome copies by ~1 log. When dasatinib at 0.5 mg/kg/day was delivered together with imatinib mesylate, the viral load was nearly identical to that seen with dasatinib alone at 0.5 mg/kg/day. These data suggest that dasatinib itself, at 0.5 mg/kg/day, had little impact on viral load but that at this dose, the drug could abrogate the protective effects of imatinib mesylate. Notably, when dasatinib at 0.05 mg/kg/day was delivered together with imatinib mesylate, the beneficial effects of the latter drug were apparent, though diminished by ~1 log. Taken together, these data indicate that dasatinib treatment is unlikely to afford protection to lethally infected mice and indeed may have an immunosuppressive activity, likely due to inhibition of Src family kinases.

Previous work demonstrated that imatinib mesylate was capable of protecting mice from a lethal challenge when administered prophylactically. We next sought to extend this observation and to test the therapeutic potential of the drug. To do this, mice were challenged with 2×10^4 PFU of VacV IHD-J i.n. (the LD_{100}). Mice were implanted with osmotic pumps to deliver imatinib mesylate (200 mg/kg/day) 24 h prior to infec-

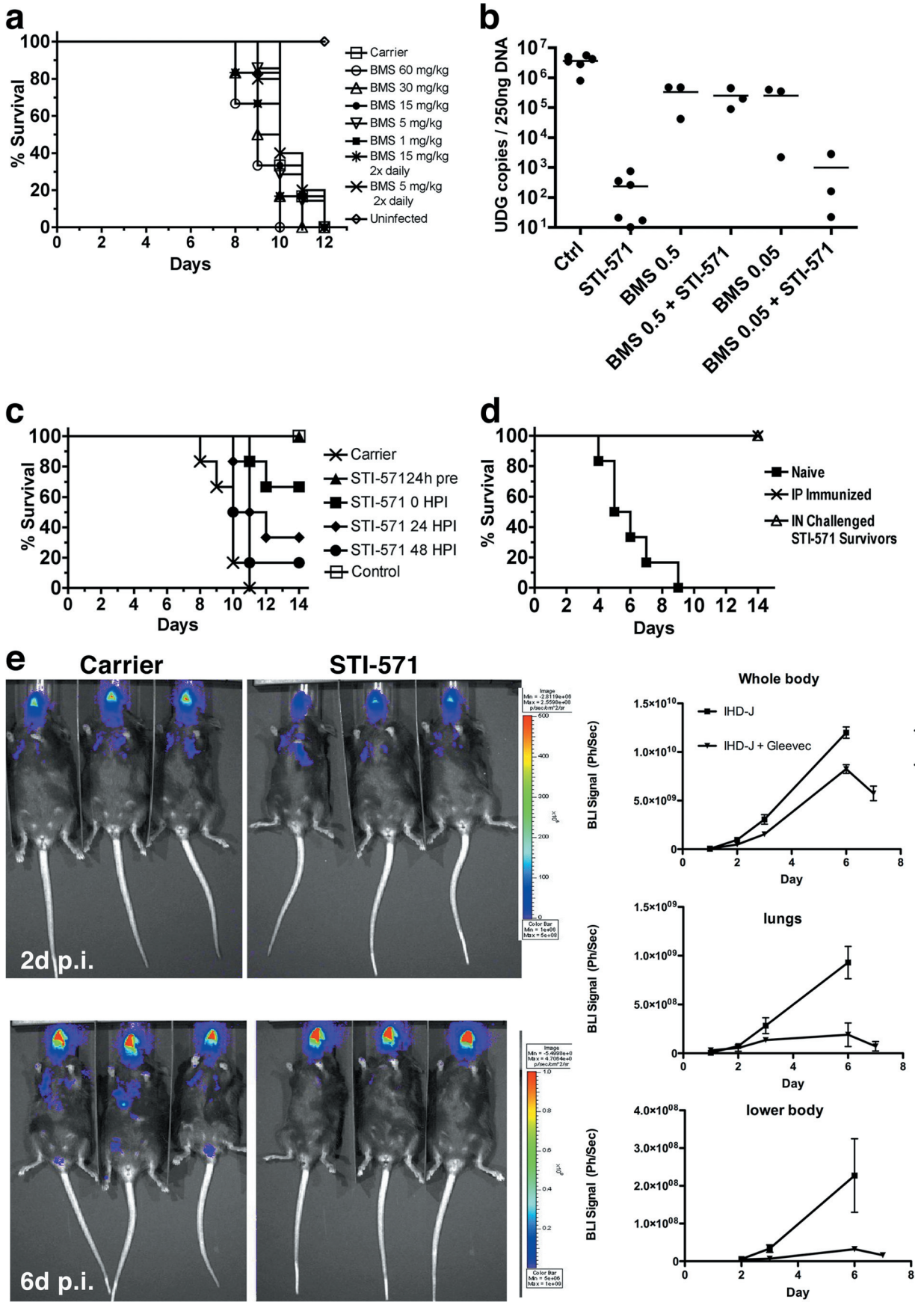
a
% Survival
Days
Carrier
BMS 60 mg/kg
BMS 30 mg/kg
BMS 15 mg/kg
BMS 5 mg/kg
BMS 1 mg/kg
BMS 15 mg/kg 2x daily
BMS 5 mg/kg 2x daily
Uninfected
b
UDG copies / 250ng DNA
Ctrl
STI-571
BMS 0.5
BMS 0.5 + STI-571
BMS 0.05
BMS 0.05 + STI-571
c
% Survival
Days
Carrier
STI-57124h pre
STI-571 0 HPI
STI-571 24 HPI
STI-571 48 HPI
Control
d
% Survival
Days
Naive
IP Immunized
IN Challenged STI-571 Survivors
e
Carrier
STI-571
2d p.i.
6d p.i.
Whole body
lungs
lower body
BLI Signal (Ph/Sec)
IHD-J
IHD-J + Gleevec
Day

tion, at the time of infection, or 24 or 48 h postinfection. In accordance with previous reports (24), all mice treated with drug prior to infection survived (Fig. 6c). Administration of drug at the time of or following infection resulted in significant survival, though the percentage was lower than that seen with pretreatment and decreased as the time following inoculation was extended. Together, these data suggest that imatinib mesylate has a protective effect whether delivered prophylactically or in a therapeutic context.

We next tested whether imatinib mesylate interfered with the acquisition of protective immune memory. To do this, mice previously challenged with the LD_{100} and treated with imatinib mesylate were allowed to rest for 10 to 12 weeks ("STI-571 survivors"). The mice were then challenged with 1×10^8 PFU of IHD-J i.p. As controls, mice were inoculated i.p. with 2×10^4 PFU IHD-J, a nonlethal inoculum, and allowed to rest for 10 to 12 weeks before being rechallenged with 1×10^8 PFU of IHD-J IP ("immunized" mice). A control group of naïve age-matched mice was also challenged i.p. with 1×10^8 PFU of IHD-J ("naïve" mice). As shown in Fig. 6d, naïve mice all succumbed within 4 to 9 days, whereas all imatinib mesylate survivors and immunized mice remained viable. Together, these data indicate that administration of imatinib mesylate does not interfere with the acquisition of protective immune memory.

To quantify the effect of imatinib mesylate on dissemination *in vivo*, mice were infected with IHD-J Luc, a strain engineered to express firefly luciferase. Mice were infected intranasally with 2×10^2 PFU IHD-J Luc and imaged for up to 7 days postinfection. Viral gene expression, which correlates with replication, was determined as luciferase activity, measured as the intensity of luminescence emitted following injection of luciferin. The images demonstrate significant luciferase activity in the nasopharyngeal tract 2 days following infection for both groups of mice (Fig. 6e). By 6 days of infection, the luciferase activity in the carrier-treated mice was evident throughout the body cavity, with high levels in the lungs and genitals. In the mice treated with imatinib mesylate, luciferase activity was restricted to the nasopharyngeal area. Quantitation of luciferase activity in the body as a whole indicated lower levels upon treatment with drug, with much more dramatic differences evident in the lower body and lungs (Fig. 6e, right panels). Together, these data indicate that imatinib mesylate protects mice from intranasal challenge by limiting spread of the virus from the site of initial infection to distal tissues.

DISCUSSION

Studies using VacV have led to a comprehensive understanding of orthopoxvirus replication, dissemination, and pathogenesis. Additionally, VacV, VarV, and MPX share 98% sequence homology. However, some variance exists among poxvirus strains and clades with respect to the precise mechanisms of dissemination. For example, different strains of VarV exhibit distinct plaque phenotypes *in vitro* and different mortality profiles *in vivo* (20). Given the potential clinical significance of VarV and MPX, we assessed whether the mode of dissemination was conserved between these viruses and VacV. Our data demonstrate that VarV and MPX are capable of inducing actin tails in a manner analogous to that of VacV. All of these viruses localize host factors known to regulate actin polymerization, such as Grb-2 and Nck. Like VacV, VarV and MPX also appear to utilize Src and Abl family tyrosine kinases in a redundant fashion (24). Of potential importance from a clinical perspective, actin tails formed by VacV, MPX, and VarV are similarly sensitive to Src and Abl family tyrosine kinase inhibitors. In plaque assays, dasatinib and PD-166326 reduced the sizes of plaques and comets, whereas imatinib mesylate reduced comet size without diminishing plaque size. The findings of EEV assays were generally consistent with those of the comet assay, with one exception. Although imatinib mesylate inhibited comet formation by VarV-BSH, VarV-SLN, MPX, and VacV, the drug appeared to have less dramatic effects in EEV assays with MPX. Because PD-166326 and dasatinib were effective in both the comet and EEV assays with MPX and because the comet assay was consistent across all strains tested, we cannot rule out that adsorption of EEV to infected cells or incomplete neutralization of IMV may contribute to apparent quantitative differences in EEV assays.

Drugs that affect poxvirus replication or spread are important to mollify symptoms associated with vaccination or for smallpox or monkeypox virus infections in individuals for whom vaccination poses a significant risk or would prove ineffective. The therapies currently approved or used on the investigational level for poxvirus infections are vaccinia immune globulin (VIG) (5, 6) and cidofovir, a DNA polymerase inhibitor (3). However, the efficacy of VIG in late-stage infections is limited, and while effective, cidofovir causes severe renal toxicity at the doses required and must be administered with intravenous hydration and in conjunction with probenecid, a renal tubular blocker that is also not without complications (14). It is unlikely that this regimen could be implemented to

FIG. 6. Effects of tyrosine kinase inhibitors on VacV infection in mice. (a) Beginning 24 h prior to infection, 6-week-old C57BL/6 mice received PBS (carrier) or dasatinib (BMS-354825) continuously via a subcutaneous osmotic pump or twice daily by i.p. injection, at the concentrations indicated. Mice were infected i.n. with 2×10^4 PFU VacV IHD-J ($n = 6$ mice per condition). (b) One day prior to infection, mice were implanted with subcutaneous osmotic pumps to deliver imatinib mesylate (STI-571; 200 mg/kg/day), dasatinib (BMS-354825; 0.5 mg/kg/day or 0.05 mg/kg/day), or both drugs in a single pump. Control mice received PBS (carrier). Four days after i.p. infection, viral genome copies were quantified by quantitative PCR. Each mouse is represented as a data point. Each horizontal line represents the median number of viral genome copies for each condition. (c) Effects of imatinib mesylate (STI-571; 200 mg/kg/day) delivered 24 h before, at the time of (0 h), or 24 or 48 h after i.n. infection with 2×10^4 PFU VacV IHD-J. Carrier mice received PBS. Control mice were left uninfected. (d) Age-matched naïve controls, i.p. immunized mice, or mice treated with imatinib mesylate (STI-571; 200 mg/kg/day) that survived a previous challenge with the LD_{100} (2×10^4 PFU) of VacV IHD-J were injected i.p. with 10^8 PFU of VarV IHD-J. The percent survival is plotted as a function of time after infection. (e) Six-week-old C57BL/6 mice were infected i.n. with 2×10^2 PFU IHD-J Luc, and luciferase activity was imaged at 2 days (2d) or 6 days (6d) postinfection. Animals received either PBS carrier or imatinib mesylate (STI-571; 200 mg/kg/day).

successfully treat a significant number of infected individuals. Another drug, ST-246, blocks formation of CEV and EEV and has shown efficacy in mouse and nonhuman primate models of poxvirus infection (12, 23), though it apparently engenders resistance. ST-246 is currently in human trials.

Would tyrosine kinase inhibitors such as dasatinib and imatinib mesylate prove efficacious *in vivo*? The *in vivo* shortcomings of dasatinib stand in stark contrast to its apparent promise based on *in vitro* assays. Despite robust *in vitro* effects on plaque size and comets, dasatinib neither reduces viral loads nor protects mice from lethal challenge. During the course of our experiments, the European Medicines Agency reported immunotoxicity for dasatinib (10). Specifically, treatment with a dose of 25 mg/kg, but not 15 mg/kg, delivered once daily prevents graft rejection in a murine cardiac transplant model. Furthermore, dasatinib inhibits murine splenic T-cell proliferation and induces lymphoid depletion of the thymus and spleen. These data are in accordance with our observation that dasatinib induces splenopenia and suppresses the effects of imatinib mesylate on dissemination of VacV. Taken together, these data indicate that immunotoxicity of dasatinib likely accounts for its failure to provide benefit for poxvirus infections. Unfortunately, we were unable to define a concentration or dosing regimen that would minimize immunosuppressive effects yet still abrogate viral dissemination.

The most likely explanation for the immunosuppressive effects of dasatinib is the inhibition of Src family kinases rather than Abl family kinases. In particular, Fyn and other Src family tyrosine kinases have been implicated in various aspects of the immune response, including innate and antigen signaling, phagocytosis, and T- and B-cell development (15, 18, 33). Dasatinib also inhibits Abl family kinases more potently than imatinib mesylate does. However, our data with the latter suggest that inhibition of Abl family kinases *per se* likely does not contribute to significant immunosuppression: imatinib mesylate did not prevent acquisition of protective immunity to poxviruses, and the drug is well tolerated in human patients, who show little increased incidence of infection (35). Furthermore, we demonstrated the ability of imatinib mesylate to limit dissemination of virus *in vivo*, a finding consistent with our *in vitro* data (Fig. 6). Together, these data suggest that dual Src/Abl inhibitors provide little *in vivo* benefit against microbial infections, despite their apparent efficacy *in vitro*.

In contrast to the case for dasatinib, the data presented here suggest that imatinib mesylate can provide significant protection when administered postinfection, in addition to its prophylactic effects reported previously (24). Nevertheless, the benefits decrease in a time-dependent manner following inoculation. The absence of drug during the period following inoculation may permit virus to establish infection and to spread to distal tissues. Once established in distal tissues, viral replication and actin tails may contribute to further expansion of virus, despite the addition of the drug. A similar argument may account for our observation that increasing the inoculum to 2×10^5 PFU, or 10 times the LD_{100}, overcame the protective benefit of imatinib mesylate (data not shown). Notably, the effects of imatinib mesylate on limiting dissemination were particularly evident at low viral titers (Fig. 6e), akin to the infectious dose for VarV in humans, in luciferase assays. Another factor contributing to the efficacy of imatinib mesylate following inoculation may be that drug delivered via an osmotic pump reaches therapeutic levels only after 16 to 18 h. Despite these caveats on the precise timing of its delivery, imatinib mesylate provides a significant level of protection pre- or postinfection, perhaps by allowing time for an effective immune response to develop, in a manner that does not interfere with acquisition of protective immune memory. Collectively, these data suggest that the potential utility of imatinib mesylate for treatment of poxvirus infections should be evaluated further.

In this regard, prairie dogs may offer a means to assess the therapeutic value of imatinib mesylate for MPX infections (12a). Similar to the case in the murine model, an inoculum of 5×10^4 PFU i.n. is used. However, this model is distinguished by the appearance of disseminated lesions or "pox" at 9 to 12 days postinfection, a phenotype previously observed only in primate models. In humans, pox lesions generally appear 7 to 19 days following infection and have been attributed to migration of EEV through the lymphatic system to the skin. Thus, presentation of pox in the prairie dog model recapitulates an important aspect of disease progression seen in humans but not in other small-animal models. Our data demonstrating that imatinib mesylate limits EEV release *in vitro* and dissemination *in vivo*, especially at low inoculums (Fig. 6e), suggest that this drug may have efficacy against MPX in prairie dogs and possibly primates, using rash illness progression as a disease marker, a prospect we are now testing.

Imatinib mesylate may also have utility when coadministered with other compounds under consideration as poxvirus therapeutics, such as ST-246 and cidofovir. ST-246 protects mice from lethal challenge when administered by up to 3 days postinfection (2). ST-246 acts more distally than imatinib mesylate by inhibiting F13 and interfering with IEV production and viral dissemination (36). Notably, however, variants resistant to ST-246 have been described that result from a single base change in F13L (36). Similarly, resistance to cidofovir is conferred by point mutations in E9L, the DNA polymerase gene (1). In contrast, imatinib mesylate is less likely to engender resistant mutants because it targets host kinases. Moreover, when coadministered, imatinib mesylate may reduce viral loads and decrease the probability of developing mutants resistant to ST-246 or cidofovir.

In summary, we describe a conserved mode of dissemination within the orthopoxvirus family and the mechanism of actin tail formation and EEV release by MPX and VarV. In addition, we show that dual Src/Abl inhibitors effectively limit both actin tail-based motility and EEV release *in vitro*. However, their utility against poxvirus infections *in vivo* is precluded by their immunosuppressive activity. In contrast, we show that imatinib mesylate can be used in a therapeutic context and does not interfere with the acquisition of immune memory, which may warrant further testing of this or related drugs in animal models of poxvirus infection.

ACKNOWLEDGMENTS

This work was supported by NIH grant R01A107246201A2 to D.K.

We thank Jay Hooper (USAMRIID), Bernard Moss (NIH), and Stewart Isaacs (University of Pennsylvania) for sharing antibodies.

P.M.R., S.H.T., I.K.D., and D.K. conceived and designed experiments. P.M.R., V.A.O., S.H.T., and S.K.S. performed the experiments. W.B. contributed reagents, materials, and analysis tools. P.M.R. and D.K. analyzed the data. P.M.R. and D.K. wrote the paper.

D.K. and P.M.R. are entitled to royalties derived from the sale of products by Inhibikase Pharmaceuticals related to the research described in this paper. The terms of this arrangement have been reviewed and approved by Emory University, in accordance with its conflict-of-interest policies.

REFERENCES

1. **Becker, M. N., M. Obraztsova, E. R. Kern, D. C. Quenelle, K. A. Keith, M. N. Prichard, M. Luo, and R. W. Moyer.** 2008. Isolation and characterization of cidofovir resistant vaccinia viruses. Virol. J. **5:**58.
2. **Berhanu, A., D. S. King, S. Mosier, R. Jordan, K. F. Jones, D. E. Hruby, and D. W. Grosenbach.** 2009. ST-246(R) inhibits in vivo poxvirus dissemination, virus shedding, and systemic disease manifestation. Antimicrob. Agents Chemother. **53:**4999–5009.
3. **Bray, M., M. Martinez, D. F. Smee, D. Kefauver, E. Thompson, and J. W. Huggins.** 2000. Cidofovir protects mice against lethal aerosol or intranasal cowpox virus challenge. J. Infect. Dis. **181:**10–19.
4. **Carter, G. C., G. Rodger, B. J. Murphy, M. Law, O. Krauss, M. Hollinshead, and G. L. Smith.** 2003. Vaccinia virus cores are transported on microtubules. J. Gen. Virol. **84:**2443–2458.
5. **CDC.** 2003. Smallpox vaccination and adverse reactions. Guidance for clinicians. MMWR Recomm. Rep. **52**(RR-4)**:**1–28.
6. **CDC.** 2001. Vaccinia (smallpox) vaccine recommendations of the Advisory Committee on Immunization Practices (ACIP), 2001. MMWR Recomm. Rep. **50**(RR-10)**:**1–25.
7. **CDC.** 2003. Multistate outbreak of monkeypox—Illinois, Indiana, and Wisconsin, 2003. MMWR Morb. Mortal. Wkly. Rep. **52:**537–540.
8. **Chen, Z., P. Earl, J. Americo, I. Damon, S. K. Smith, F. Yu, A. Sebrell, S. Emerson, G. Cohen, R. J. Eisenberg, I. Gorshkova, P. Schuck, W. Satterfield, B. Moss, and R. Purcell.** 2007. Characterization of chimpanzee/human monoclonal antibodies to vaccinia virus A33 glycoprotein and its variola virus homolog in vitro and in a vaccinia virus mouse protection model. J. Virol. **81:**8989–8995.
9. **Damon, I. K.** 2006. Poxviruses, p. 2947–2976. *In* B. N. Fields et al. (ed.), Fields virology, 5th ed. Raven Press, New York, NY.
10. **European Medicines Agency.** 2006. Sprycel European public assessment report, p. 46. European Medicines Agency, London, United Kingdom.

10a. **Frischknecht, F., V. Moreau, S. Röttger, S. Gonfloni, I. Reckmann, G. Superti-Furga, and M. Way.** 1999. Actin-based motility of vaccinia virus mimics receptor tyrosine kinase signalling. Nature **401:**926–929.

11. **Hollinshead, M., G. Rodger, H. Van Eijl, M. Law, R. Hollinshead, D. J. Vaux, and G. L. Smith.** 2001. Vaccinia virus utilizes microtubules for movement to the cell surface. J. Cell Biol. **154:**389–402.
12. **Huggins, J., A. Goff, L. Hensley, E. Mucker, J. Shamblin, C. Wlazlowski, W. Johnson, J. Chapman, T. Larsen, N. Twenhafel, K. Karem, I. K. Damon, C. M. Byrd, T. C. Bolken, R. Jordan, and D. Hruby.** 2009. Nonhuman primates are protected from smallpox virus or monkeypox virus challenges by the antiviral drug ST-246. Antimicrob. Agents Chemother. **53:**2620–2625.

12a. **Hutson, C. L., V. A. Olson, D. S. Carroll, J. A. Abel, C. M. Hughes, Z. H. Braden, S. Weiss, J. Self, J. E. Osorio, P. N. Hudson, M. Dillon, K. L. Karem, I. K. Damon, and R. L. Regnery.** 2009. A prairie dog animal model of systemic orthopoxvirus disease using West African and Congo Basin strains of monkeypox virus. J. Gen. Virol. **90:**323–333.

13. **Kalman, D., O. D. Weiner, D. L. Goosney, J. W. Sedat, B. B. Finlay, A. Abo, and J. M. Bishop.** 1999. Enteropathogenic E. coli acts through WASP and Arp2/3 complex to form actin pedestals. Nat. Cell Biol. **1:**389–391.
14. **Lacy, S. A., M. J. Hitchcock, W. A. Lee, P. Tellier, and K. C. Cundy.** 1998. Effect of oral probenecid coadministration on the chronic toxicity and pharmacokinetics of intravenous cidofovir in cynomolgus monkeys. Toxicol. Sci. **44:**97–106.
15. **Lowell, C. A.** 2004. Src-family kinases: rheostats of immune cell signaling. Mol. Immunol. **41:**631–643.
16. **Mortimer, P. P.** 2003. Can postexposure vaccination against smallpox succeed? Clin. Infect. Dis. **36:**622–629.
17. **Moss, B.** 2006. Poxviridae: the viruses and their replication, p. 2905–2946. *In* B. N. Fields et al. (ed.), Fields virology, 5th ed. Raven Press, New York, NY.
18. **Mustelin, T., and K. Tasken.** 2003. Positive and negative regulation of T-cell activation through kinases and phosphatases. Biochem. J. **371:**15–27.
19. **National Research Council.** 1999. Assessment of future scientific needs for live variola virus. National Academy Press, Washington, DC.

19a. **Newsome, T., F. Frischknecht, and M. Way.** 2006. Abl collaborates with Src family kinases to stimulate actin-based motility of vaccinia virus. Cell. Microbiol. **8:**233.

20. **Olson, V. A., K. L. Karem, S. K. Smith, C. M. Hughes, and I. K. Damon.** 2009. Smallpox virus plaque phenotypes: genetic, geographical and case fatality relationships. J. Gen. Virol. **90:**792–798.
21. **Parker, S., A. Nuara, R. M. Buller, and D. A. Schultz.** 2007. Human monkeypox: an emerging zoonotic disease. Future Microbiol. **2:**17–34.
22. **Ploubidou, A., V. Moreau, K. Ashman, I. Reckmann, C. Gonzalez, and M. Way.** 2000. Vaccinia virus infection disrupts microtubule organization and centrosome function. EMBO J. **19:**3932–3944.
23. **Quenelle, D. C., R. M. Buller, S. Parker, K. A. Keith, D. E. Hruby, R. Jordan, and E. R. Kern.** 2007. Efficacy of delayed treatment with ST-246 given orally against systemic orthopoxvirus infections in mice. Antimicrob. Agents Chemother. **51:**689–695.
24. **Reeves, P. M., B. Bommarius, S. Lebeis, S. McNulty, J. Christensen, A. Swimm, A. Chahroudi, R. Chavan, M. B. Feinberg, D. Veach, W. Bornmann, M. Sherman, and D. Kalman.** 2005. Disabling poxvirus pathogenesis by inhibition of Abl-family tyrosine kinases. Nat. Med. **11:**731–739.
25. **Rietdorf, J., A. Ploubidou, I. Reckmann, A. Holmstrom, F. Frischknecht, M. Zettl, T. Zimmermann, and M. Way.** 2001. Kinesin-dependent movement on microtubules precedes actin-based motility of vaccinia virus. Nat. Cell Biol. **3:**992–1000.
26. **Scaplehorn, N., A. Holmstrom, V. Moreau, F. Frischknecht, I. Reckmann, and M. Way.** 2002. Grb2 and Nck act cooperatively to promote actin-based motility of vaccinia virus. Curr. Biol. **12:**740–745.
27. **Smith, G. L., B. J. Murphy, and M. Law.** 2003. Vaccinia virus motility. Annu. Rev. Microbiol. **57:**323–342.
28. **Smith, G. L., A. Vanderplasschen, and M. Law.** 2002. The formation and function of extracellular enveloped vaccinia virus. J. Gen. Virol. **83:**2915–2931.
29. **Smith, S. K., V. A. Olson, K. L. Karem, R. Jordan, D. E. Hruby, and I. K. Damon.** 2009. In vitro efficacy of ST246 against smallpox and monkeypox. Antimicrob. Agents Chemother. **53:**1007–1012.
30. **Swedlow, J. R., J. W. Sedat, and D. A. Agard.** 1997. Deconvolution in optical microscopy, p. 284–307. *In* P. A. Jansson (ed.), Deconvolution of images and spectra. Academic Press, Inc., San Diego, CA.
31. **Swimm, A., B. Bommarius, Y. Li, D. Cheng, P. Reeves, M. Sherman, D. Veach, W. Bornmann, and D. Kalman.** 2004. Enteropathogenic Escherichia coli use redundant tyrosine kinases to form actin pedestals. Mol. Biol. Cell **15:**3520–3529.
32. **Tolomeo, M., F. Dieli, N. Gebbia, and D. Simoni.** 2009. Tyrosine kinase inhibitors for the treatment of chronic myeloid leukemia. Anticancer Agents Med. Chem. **9:**853–863.
33. **Tsygankov, A. Y., S. Mahajan, J. E. Fincke, and J. B. Bolen.** 1996. Specific association of tyrosine-phosphorylated c-Cbl with Fyn tyrosine kinase in T cells. J. Biol. Chem. **271:**27130–27137.
34. **Ward, B. M., and B. Moss.** 2001. Vaccinia virus intracellular movement is associated with microtubules and independent of actin tails. J. Virol. **75:**11651–11663.
35. **Wolf, D., and H. Rumpold.** 2009. A benefit-risk assessment of imatinib in chronic myeloid leukaemia and gastrointestinal stromal tumours. Drug Saf. **32:**1001–1015.
36. **Yang, G., D. C. Pevear, M. H. Davies, M. S. Collett, T. Bailey, S. Rippen, L. Barone, C. Burns, G. Rhodes, S. Tohan, J. W. Huggins, R. O. Baker, R. L. Buller, E. Touchette, K. Waller, J. Schriewer, J. Neyts, E. DeClercq, K. Jones, D. Hruby, and R. Jordan.** 2005. An orally bioavailable antipoxvirus compound (ST-246) inhibits extracellular virus formation and protects mice from lethal orthopoxvirus challenge. J. Virol. **79:**13139–13149.